

## Advective Coalescence in Chaotic Flows

Takashi Nishikawa

*Department of Mathematics, Arizona State University, Tempe, Arizona 85287*

Zoltán Toroczkai

*Theoretical Division and Center for Nonlinear Studies, Los Alamos National Laboratory,  
Mailstop B258, Los Alamos, New Mexico 87545*

Celso Grebogi

*Instituto de Física, Universidade de São Paulo, Caixa Postal 66318, 05315-970 São Paulo, SP, Brazil  
(Received 14 September 2000; revised manuscript received 22 March 2001; published 29 June 2001)*

We investigate the reaction kinetics of small spherical particles with inertia, obeying coalescence type of reaction,  $B + B \rightarrow B$ , and being advected by hydrodynamical flows with time-periodic forcing. In contrast to passive tracers, the particle dynamics is governed by the strongly nonlinear Maxey-Riley equations, which typically create chaos in the spatial component of the particle dynamics, appearing as filamental structures in the distribution of the reactants. Defining a stochastic description supported on the natural measure of the attractor, we show that, in the limit of slow reaction, the reaction kinetics assumes a universal behavior exhibiting a  $t^{-1}$  decay in the amount of reagents, which become distributed on a subset of dimension  $D_2$ , where  $D_2$  is the correlation dimension of the chaotic flow.

DOI: 10.1103/PhysRevLett.87.038301

PACS numbers: 82.40.Bj, 47.52.+j, 47.70.Fw, 87.23.Cc

The coupling between the generically nonlinear character of environmental flows and the spatial distribution of growing and (temporally) evolving populations (such as planktons) advected by these flows attracted considerable interest recently [1–3]. The flow in fluid environments of large extensions, such as oceans, presents imperfect mixing properties. This is largely due to the fact that the body of these fluids is striated by running currents, by the vortices and eddies generated by obstacles such as large rocks or islands and peninsulas, or by the winds blowing across the fluids' surface [4–6]. A small particle (about the size of a plankton) advected by this flow typically follows a chaotic path; i.e., it is subjected to chaotic advection. In such conditions, the spatial distribution of particle ensembles has a filamental structure [1,7]. It has recently been shown [1] that in the limit of massless passive point tracers, and open chaotic flows (for the case of closed flows see Ref. [8]), the reaction kinetics of autocatalytic reagents is entirely different from the traditional surface reaction, being singularly enhanced and catalyzed by the underlying fractal advection patterns.

Herewith, we analyze *active chaos* with an activity component that plays an important role in biological population dynamics [9], and agglomeration phenomena in environmental physics, physical chemistry, and engineering [10–12]. In crowded populations, when the local density exceeds a critical value, the mortality rate of individuals increases due to the fact that the niches they occupy (food, necessary chemicals, light) have only a finite capacity. Qualitatively, this may be modeled by *coalescence* type of reaction  $B + B \rightarrow B$ . Namely, if two individuals become closer than a given reaction range  $\sigma$ , one of them dies on an average time scale  $\tau$  that is also

defined as the average reaction lag. The reaction range  $\sigma$  represents a *crowding threshold* for the active population. When the population is made up of small particles, such as phytoplanktons which thrive in a fluid media, the fluid dynamics has a crucial role on the evolution of the population due to the local coupling between the spatial character of the reaction (the fate of the reaction depends on the neighborhood occupancy of the particles) and the chaotic fluid dynamics that is constantly stirring the population.

In this Letter, we show that for the case of finite-size particles with nonzero mass and nonzero spatial extension, chaotic behavior may appear in the physical space component of the particle dynamics, and it arises due to the dissipative nature given by the Stokes drag. This discriminating chaotic dynamics ultimately generates a nontrivial reaction kinetics which attains a universal limit for reaction lags of the order of or larger than the inverse of the largest average Lyapunov exponent. In this limit, the temporal evolution of the reaction kinetics is independent of the details of the chaotic dynamics, and even of the dimensionality of the flow. The information about dimensionality and the properties of the chaotic set are important on the level of coefficients, but not on the level of exponents. In particular, we show that, in the slow reaction limit, the total number of particles decays as  $t^{-1}$ . The coefficient of proportionality describes the spatial distribution of the reactants that is shown to occupy only a subset with fractal dimension  $D_2$  on the attractor.

We emphasize that dissipative chaotic behavior in the spatial component of the dynamics arises *solely* from the Stokes drag in the advection dynamics and from the time dependence of the underlying flow (which can be as simple

as a periodic flow). The massless passive point-tracer approach [1] is a somewhat oversimplified picture of the reality. Since the tracers in real flows often cannot be considered to be massless point particles, it is important to address the question of finite-size effects on the particle dynamics [13]. These effects are the force exerted on the particle by the undisturbed flow, the buoyancy force, the Stokes drag, the added mass effect, and the Basset-Boussinesq history term including the Faxén corrections. The equations, including these effects at low Reynolds number, were explicitly given by Maxey and Riley [14,15].

To illustrate the finite-size effects on the advective coalescence problem, we choose one of the simplest incompressible cellular flow [16–18] with periodic time dependence, given by the stream function

$$\psi(x_1, x_2) = [1 + k \sin(\omega t)]U_0L \sin(x_1/L) \sin(x_2/L), \quad (1)$$

where  $U_0$  is the velocity amplitude,  $\pi L$  is the size of the vortex cell,  $k$  and  $\omega$  are the amplitude and angular frequency of the temporal oscillation of the flow field, respectively. The contour plot of the stream function is shown in Fig. 1. The fluid element's velocity  $\mathbf{u}$  at point  $(x_1, x_2)$  is then obtained from  $\mathbf{u} = \nabla \times \boldsymbol{\psi}$ , where  $\boldsymbol{\psi} = (0, 0, \psi)$ . The time-independent version of the flow dynamics ( $k = 0$ ) was first considered by Stommel [5] as a simple model to describe the distribution of planktons resulting from the cellular motion induced by winds in lakes and oceans, often called the Langmuir circulation [4]. The effects of finite-size particles of this particular flow, without forcing ( $k = 0$ ), were analyzed in great detail by Maxey [16]. The asymptotic particle trajectories are well defined smooth curves extending from cell to cell. The situation becomes completely different, and the flow dynamics inherently

chaotic, if time dependence is also introduced. Here we shall not reproduce the derivation but just present the final equations of motion in dimensionless parameters as [18]

$$\frac{d\mathbf{V}}{dt} = A[\mathbf{u} - \mathbf{V} + \mathbf{W}] + R\left(\mathbf{u} + \frac{\mathbf{V}}{2}\right) \cdot \nabla \mathbf{u} + \frac{3R}{2} \frac{\partial \mathbf{u}}{\partial t}, \quad (2)$$

where  $\mathbf{V}$  is the velocity of the particle (in units of  $U_0$ ), and  $\mathbf{u} = \mathbf{u}(\mathbf{Y}(t))$  is the velocity field (in units of  $U_0$ ) at the position (in units of  $L$ )  $\mathbf{Y}(t)$  of the particle. The (dimensionless) parameters  $A$ ,  $R$ , and  $\mathbf{W}$  can be expressed in terms of  $L$ ,  $U_0$ , the particle radius  $a$ , the particle mass  $m_p$ , the fluid's viscosity  $\mu$ , the fluid mass displaced by the particle  $m_f$ , and the gravitational acceleration  $g$ . The parameter  $A = 6\pi a \mu L / [U_0(m_p + m_f/2)]$  represents the inertia effect (larger values imply smaller inertia). The limit of  $A \rightarrow \infty$  is the tracer particle limit. The buoyancy parameter is  $R = m_f / (m_p + m_f/2)$ . The regime  $R > 2/3$  describes bubbles, and  $R < 2/3$  corresponds to aerosols. The terminal velocity of the particle in still fluid is given by  $\mathbf{W} = (m_p - m_f)\mathbf{g} / (6\pi a \mu)$ .

Because of the spatial periodicity of the flow field, the dynamics of the particles can be considered to be restricted to a basic cell  $[0, 2\pi] \times [0, 2\pi]$  with periodic boundary conditions. We consider the stroboscopic mapping of the flow at the period of the flow field. Throughout the simulations we keep the parameters fixed at the following values:  $k = 2.72$ ,  $\omega = \pi$ ,  $A = 3.2$ ,  $R = 1$ , and  $\mathbf{W} = (0, -0.8)$ . The time on the stroboscopic map is measured in units of the flow's period,  $T = 2\pi/\omega = 2$ . We find that in this bubble regime, where the particles are lighter than the surrounding fluid, with large enough amplitude of the forcing (large enough that the rotation of the vortices change their direction periodically) the attractor is chaotic and strange [19], as shown in Fig. 1. This fact is supported by the computed largest average Lyapunov exponent,  $\Lambda_+ \approx 0.02$ , and the box-counting dimension  $D_0 \approx 1.62$ .

The activity, given by the coalescence process  $B + B \rightarrow B$ , is implemented in the following way. On a grid of size  $\varepsilon$ , we choose a set of boxes that covers the chaotic attractor and put a particle at the center of each box. There are a total of  $N(\varepsilon)$  boxes covering the attractor. We evolve forward in time each particle in the system by integrating Eq. (2) for some fixed time  $\tau$  (which is measured in units of  $T$ ), and put the particle in the box at the end point of the trajectory. If two or more particles end up in the same box, the first one to arrive remains in it, and the others are removed from the system. We then repeat this procedure to obtain the time evolution of the coalescence process. For simplicity, we choose  $\sigma = \varepsilon = 5 \times 10^{-3}$  to be the crowding threshold. Actually, the reaction does not necessarily take place for all the particles at the same time but rather randomly in time. We approximate this situation by regarding  $\tau$  as the mean reaction time of a particle. This approximation does not have a substantial effect on the qualitative results [20].

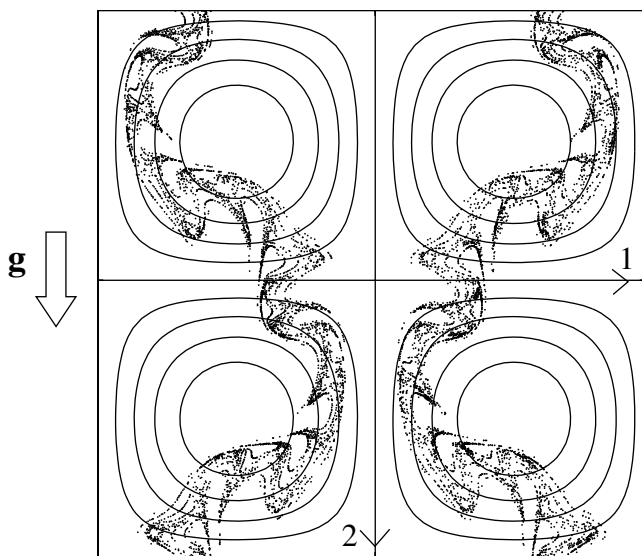


FIG. 1. Contour plot for the stream function in Eq. (1) (continuous closed curves), and the chaotic attractor (dots) for the stroboscopic map of the flow generated using Eq. (2).

In the simulations, we monitor the number density of the particles defined as  $n(t) = N(t)/N_0$ , where  $N(t)$  is the total number of particles at time  $t$  in the  $N_0 = N(\varepsilon)$  boxes covering the attractor. A typical result from the simulations for the number density  $n(t)$  is shown in Fig. 2 on a log-log scale for two  $\tau$  values,  $\tau = 2$  (the + symbols) and  $\tau = 10$  (the × symbols). We find that the asymptotic temporal behavior is given by  $n(t) \sim t^{-1}$ , which seems to be also closely obeyed even for smaller  $\tau$  values (such as  $\tau = 2$ , where the exponent of the decay is  $\sim -0.9$ ).

In the following, we show analytically that this type of behavior, in the limit of slow reaction (large  $\tau$ ), is, in fact, a consequence of the universality of the coalescence reaction kinetics of the system. In order to derive that, we first recall that the natural invariant measure of an  $\varepsilon$  box is the probability for the trajectory to visit that box. Based on that, on a statistical level, we may approximate the dynamics of the flow by a *stochastic process* of simply shuffling the particles among the boxes covering the attractor, according to the probability given by the natural measure of the chaotic dynamics. Let  $p_1, p_2, \dots, p_N$  be the natural measure of each particular  $\varepsilon$  box covering the attractor (the natural measure is normalized,  $\sum_{j=1}^N p_j = 1$ ). The *shuffling* step is defined as follows: take the image of the set of  $N(t)$  particles such that the image of a particular particle is in box  $i$  with probability  $p_i$ . Notice that this is a parallel updating process. After each shuffling, *coalescence* is imposed in every box containing two or more particles. If we focus on one step of this stochastic process (shuffling + coalescence), we may ask the following question: What is the expected number of boxes that are not empty after one step of the stochastic process, if at the beginning of the step we had  $m$  particles in  $m$  different boxes? Using combinatorial analysis, we infer that the probability  $p(m, k)$  of ending up with  $k$  nonempty boxes is given by the sum of

$$\frac{m!}{m_1! \dots m_k!} p_{i_1}^{m_1} \dots p_{i_k}^{m_k}$$

over all possible sets of integers  $i_1, \dots, i_k$  chosen from  $\{1, 2, \dots, N\}$  without replacement and all possible sets of integers  $m_1, \dots, m_k$  such that  $1 \leq m_1, \dots, m_k < m$  and  $m_1 + \dots + m_k = m$ . The sum can be reduced to

$$p(m, k) = \sum_{j=1}^k (-1)^{k-j} \binom{N-j}{k-j} \sum_{\mathbf{l}_j} (p_{l_1} + \dots + p_{l_j})^m, \quad (3)$$

if  $k \leq m$ , and  $p(m, k) = 0$  otherwise. The second sum is taken over all  $\binom{N}{j}$  possible choices of  $j$  numbers  $\{l_1, l_2, \dots, l_j\} (= \mathbf{l}_j)$  from  $\{1, 2, \dots, N\}$ . In particular, if one would have a uniform measure, i.e.,  $p_1 = \dots = p_N = 1/N$ , this distribution would become related to the Stirling numbers of the second kind  $S(m, k)$ :  $p(m, k) = (N)_m N^{-m} S(m, k)$ , where  $(N)_m = N(N-1) \dots (N-m+1)$  and  $S(m, k) = \frac{1}{k!} \sum_{j=0}^k (-1)^j \binom{k}{j} (k-j)^m$ . From (3) we can compute the average number density of nonempty boxes as

$$\frac{\langle k \rangle_m}{N} = \frac{1}{N} \sum_{k=1}^N k p(m, k) = 1 - \frac{1}{N} \sum_{i=1}^N (1 - p_i)^m. \quad (4)$$

However, the process is an iterative one: one starts with  $m$  particles, then we obtain  $m_1 \leq m$  after one step,  $m_2 \leq m_1$  after two steps, etc. This decay process can be described by (4) if one replaces the exponent  $m$  on the right-hand side of Eq. (4) with  $Nn(t)$  and on the left-hand side, by definition, with  $n(t+1)$ , yielding the map

$$n(t+1) = 1 - \frac{1}{N} \sum_{i=1}^N (1 - p_i)^{Nn(t)}. \quad (5)$$

Choosing  $n(0) = 1$ , the time evolution of the number density  $n(t)$  obtained from Eq. (5) is plotted in Fig. 2 (continuous line). Notice the excellent agreement with \* symbols that represent the average of 20 runs of the direct simulation of the stochastic process consisting of random shuffling and coalescence, which we have described above. Since  $N = N(\varepsilon) \gg 1$ ,  $p_i \ll 1$  for all the boxes, we may expand  $(1 - p_i)^{Nn(t)}$  up to the second order in  $p_i$ , which yields

$$\frac{dn}{dt} = -C[n(t)]^2, \quad (6)$$

where  $C = (N/2) \sum_{i=1}^N p_i^2$ . The solution of Eq. (6) [if  $n(0) = 1$ ] is just  $(Ct + 1)^{-1}$ ; i.e., it is  $\sim t^{-1}$  for long times, as observed in our simulations. The coefficient  $C$  can simply be related to the set of dimensions [21].  $C = \frac{\chi(0)\chi(2)}{2} \sim \varepsilon^{D_2 - D_0}$ , where  $D_q = \lim_{\varepsilon \rightarrow 0} \frac{1}{q-1} \frac{\ln \chi(q)}{\ln \varepsilon}$ , and  $\chi(q) = \sum_i p_i^q$  [note that  $N = N(\varepsilon) = \chi(0)$ ].  $D_2$  is the correlation dimension.

If one looks at the number  $N(t)$  instead of the number density, one finds that the decay law for long times is

$$N(\varepsilon, t) \sim \varepsilon^{-D_2} t^{-1}. \quad (7)$$

Our results, as given in this equation, are the following: (i) the *temporal behavior* is universal and independent of

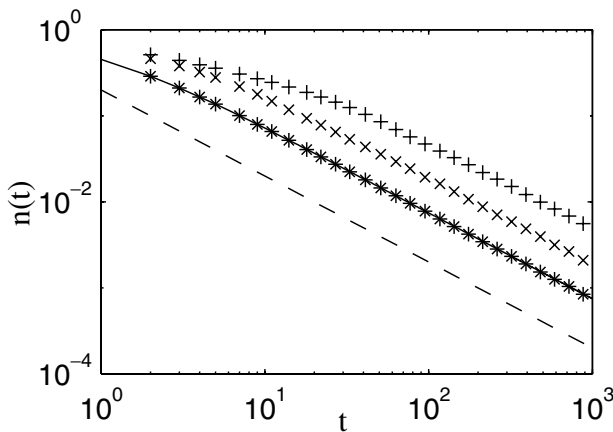


FIG. 2. The time evolution of the particle density for  $\tau = 2$  (+ symbols) and  $\tau = 10$  (× symbols). The stars (\*) correspond to the random-shuffling model using the natural measure on the attractor, and the continuous line is Eq. (5). The dashed line is a reference line of slope  $-1$ .

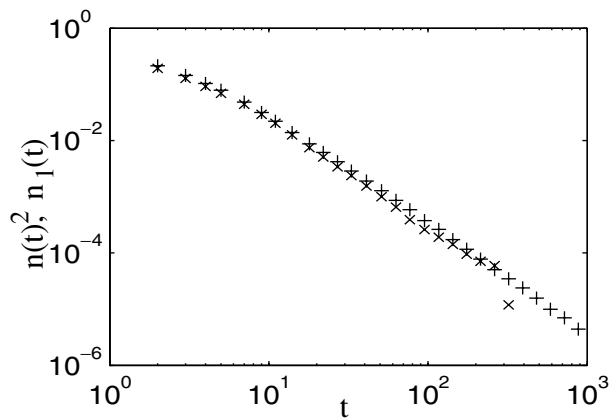


FIG. 3. Comparing  $[n(t)]^2$  ( $\times$  symbols) and  $n_1(t)$  ( $+$  symbols) at  $\tau = 10$ .

the particularities of the chaotic flow, and (ii) the surviving particles are distributed *selectively on a subset* of dimension  $D_2$  on the attractor at a given instant of time.

Based on Eq. (6), we claim that the continuum limit is the one described by the Smoluchowski equation obtained in the theory of the agglomeration reaction  $B_i + B_j \rightarrow B_{i+j}$  [11]. Although here the masses are added not annihilated, one can still use this *formalism* if one looks at certain quantities such as the total number of particles, or the number of particles that have yet to experience a reaction,  $N_1(t) \equiv n_1(t)N(t)$ . The mass index in this case is replaced by a collision index. Equation (6) is the same as the one for the total number of particles in the agglomeration process. We also evaluated the quantity  $n_1(t)$  (from the flow), which in the Smoluchowski approach obeys  $n_1 = n^2$ , at all  $t$  times. Figure 3 shows in the same plot  $n_1(t)$  and  $[n(t)]^2$  from the flow simulations for  $\tau = 10$ . Note the excellent agreement at all times  $t$  between the curves, corroborating our findings.

It is important to mention that our model described by Eq. (6) is strongly related to the experiment done by Droop [22], which verified that the nutrient-limited population growth dynamics obey the logistic equation. In the limit of low concentration, the logistic equation reduces to Eq. (6). See also Gurney and Nisbet [23]. In this Letter, however, the coefficient is related to the fractal properties of the dynamics, while in the experiment it depended on the initial concentration of the nutrient and on the properties of the growth mechanism. The validity of our model is supported by the finding by Coma *et al.* [24] which showed that there are many examples of aquatic colonies where the growth phases are separated.

In conclusion, we have shown that the dissipativity of the advection dynamics (in our example due to finite-size effects and inertia) can have drastic effects on the kinetics of the coalescence type of reaction that models the crowding phenomena of biological populations (phytoplanktons) advected in fluid flows with imperfect mixing (oceans,

lakes). The distribution of the surviving reactants selects a nontrivial subset of the attractor in the limit of slow reaction which exhibits universal behavior described by the Smoluchowski equation.

The authors acknowledge illuminating discussions with E. Ben-Naim, M. Chertkov, T. Tél, and I. Scheuring. This work was supported by ONR(Physics), DOE W-7405-ENG-36, MTA-OTKA/NSF-INT grant, and FAPESP and CNPq grants.

- [1] Z. Toroczkai, G. Károlyi, Á. Péntek, T. Tél, and C. Grebogi, Phys. Rev. Lett. **80**, 500 (1998); G. Károlyi, Á. Péntek, Z. Toroczkai, T. Tél, and C. Grebogi, Phys. Rev. E **59**, 5468 (1999); G. Károlyi, Á. Péntek, I. Scheuring, T. Tél, and Z. Toroczkai, Proc. Natl. Acad. Sci. U.S.A. **97**, 13 661 (2000).
- [2] Z. Neufeld, C. López, and P.H. Haynes, Phys. Rev. Lett. **82**, 2606 (1999); Z. Neufeld, C. López, and E. Hernández-García, and T. Tél, Phys. Rev. E **61**, 3857 (2000).
- [3] M. A. Bees, I. Mezic, and J. McGlade, Math. Comput. Simul. **44**, 527 (1999).
- [4] I. Langmuir, Science **87**, 119 (1938).
- [5] H. Stommel, J. Mar. Res. **8**, 24 (1949).
- [6] W. Munk, L. Armi, K. Fischer, and F. Zachariassen, Proc. R. Soc. London **456**, 1217 (2000).
- [7] E. R. Abraham, Nature (London) **391**, 577 (1998); J. M. Ottino, *The Kinematics of Mixing: Stretching, Chaos and Transport* (Cambridge University Press, Cambridge, 1989).
- [8] G. Metcalfe and J. M. Ottino, Phys. Rev. Lett. **72**, 2875 (1994); **73**, 212 (1994).
- [9] T. Czárán, *Spatiotemporal Models of Population and Community Dynamics* (Chapman & Hall, London, 1998).
- [10] *Topics of Current Aerosol Research*, edited by G. M. Hidy and J. R. Brock (Pergamon, New York, 1971).
- [11] M. von Smoluchowski, Z. Phys. **17**, 557 (1916).
- [12] E. Ben-Naim and P.L. Krapivsky, J. Phys. A **33**, 5465 (2000); P.L. Krapivsky and E. Ben-Naim, *ibid.* **33**, 5477 (2000).
- [13] A. Babiano, J. H. E. Cartwright, O. Piro, and A. Provenzale, Phys. Rev. Lett. **84**, 5764 (2000).
- [14] M. R. Maxey and J. J. Riley, Phys. Fluids **26**, 883 (1983).
- [15] E. E. Michaelides, J. Fluids Eng. **119**, 233 (1997).
- [16] M. R. Maxey, Phys. Fluids **30**, 1915 (1987).
- [17] M. J. Manton, Bound.-Lay. Meteorol. **6**, 487 (1974).
- [18] L. Yu, C. Grebogi, and E. Ott, *Nonlinear Structure in Physical Systems* (Springer-Verlag, New York, 1990), pp. 223–231.
- [19] C. Grebogi, E. Ott, S. Pelikan, and J. A. Yorke, Physica (Amsterdam) **13D**, 261 (1984).
- [20] G. Santoboni, T. Nishikawa, Z. Toroczkai, and C. Grebogi (to be published).
- [21] H. G. E. Hentschel and I. Procaccia, Physica (Amsterdam) **8D**, 435 (1983).
- [22] M. R. Droop, J. Phycol. **9**, 264 (1973).
- [23] W. S. C. Gurney and R. M. Nisbet, *Ecological Dynamics* (Oxford University Press, Oxford, 1998), pp. 130–131.
- [24] R. Coma, M. Ribes, J. Gili, and M. Zabala, TREE **15**, 448 (2000).